ELSEVIER

Catalysis Today 47 (1999) 133–140

CATALYSIS TODAY

Catalytic combustion of hydrocarbons with Mn and Cu-doped ceria–zirconia solid solutions

Daniela Terribile, Alessandro Trovarelli, Carla de Leitenburg*, Alessandra Primavera, Giuliano Dolcetti

Dipartimento di Scienze e Tecnologie Chimiche, Università di Udine, via Cotonificio 108, 33100 Udine, Italy

Abstract

The catalytic activity of a series of CeO_2–ZrO_2 mixed oxides in the total oxidation of methane and light hydrocarbons has been investigated. The influence of dopants like Mn and Cu has also been studied. It is shown that both MnO_x and CuO at low loading dissolve within the ceria–zirconia lattice. This strongly influences the redox behaviour of the catalysts by promoting low-temperature reduction of Ce^{4+}. In addition, the ternary oxides show better stability to repeated redox cycles, which is attributed to the presence of ZrO_2. The catalytic activity of pure CeO_2 is also enhanced in the presence of ZrO_2, reaching a maximum with $Ce_{0.92}Zr_{0.08}O_2$; a further promotion of activity is observed with the introduction of MnO_x and CuO dissolved into CeO_2–ZrO_2 lattice.

Keywords: Ceria; Zirconia; Catalytic combustion; TPR; CeO_2–ZnO_2

1. Introduction

Catalytic combustion of methane and other light hydrocarbons is receiving considerable attention in these years with the aim of providing new technological solutions for reducing emissions of air pollutants. In particular, the interest in new materials for high-temperature applications [1] and for exhaust gas treatments, especially VOC [2], has boosted research in this area. Therefore there is a strong demand for the development of new, thermally stable, low-cost materials as active and efficient catalysts for the total oxidation of hydrocarbons.

Among several types of catalysts that have been developed at various stages, particular attention is being paid to the preparation and characterization of ceria-based catalysts, and specifically CeO_2-containing mixed oxides having the fluorite structure [3].

We have recently reported that solid solutions of compositions 80%CeO_2–20%MO_2 (with M=Zr of Hf) behave as efficient and stable catalysts for the total oxidation of CH_4 [4], and several reports have appeared on the use of these materials as a base for catalysts having a high oxygen storage/transport capacity [5,6] and unusual redox properties [7]. In addition, stabilization of surface area by introduction of ZrO_2 into the CeO_2 lattice has also been reported [8]. The reason for this behaviour can be found in the efficiency of the Ce^{4+}–Ce^{3+} redox couple, which is strongly enhanced in CeO_2–ZrO_2 solid solutions due to the introduction of the smaller Zr^{4+} cation (ionic radius 0.84 Å) into the fluorite lattice of CeO_2 (ionic radius of Ce^{4+} 0.97 Å). This generates defects throughout the

*Corresponding author. Fax: +39-432-558803; e-mail: catalysis@dstc.uniud.it

0920-5861/99/$ – see front matter
PII: S0920-5861(98)00292-2

matter, which in turn, brings about an increase of the oxygen mobility and diffusion in the lattice.

In this paper we analyse in more detail the reduction and catalytic behaviour of CeO_2–ZrO_2 and Mn and Cu-doped ceria–zirconia solid solutions with the fluorite structure in the complete oxidation of C_1–C_4 hydrocarbons. In particular, we have investigated the effects of introducing Mn, and Cu into CeO_2–ZrO_2 lattice, focusing on the structural properties, thermal stability and catalytic activity. Powder X-ray diffraction, temperature-programmed reduction (TPR) and surface area measurements have been performed to pursue this aim.

2. Experimental

2.1. Materials

CeO_2 was prepared by adding slowly a solution of $Ce(NO_3)_3{\cdot}6H_2O$ (Carlo Erba) to ammonia. The resulting precipitate was washed several times with water and with acetone/toluene/acetone, and then dried at 373 K for 15 h followed by calcination at the required temperature for 2 h. Ceria–zirconia mixed oxides were synthesized by coprecipitation according to the procedure recently reported [9]. The formation of solid solutions was confirmed by X-ray diffraction measurements and combined TEM-EDX analysis [9]. Mn-doped ceria–zirconia were prepared from an aqueous solution containing stoichiometric amounts of $Ce(NO_3)_3{\cdot}6H_2O$ (C. Erba), $ZrO(NO_3)_2$ and $MnCl_2{\cdot}4H_2O$ (Aldrich). By adding this solution to ammonia a brown precipitate forms, which is then filtered, washed, and dried at 373 K for 15 h. For Cu-containing materials, $Cu(NO_3)_2{\cdot}2.5H_2O$ (Aldrich) was used and the aqueous solution containing the stoichiometric amount of the three salts was added to an aqueous solution of sodium hydroxide (1 M). The resulting yellow–brown precipitate was filtered, washed with water and then dried and calcined. The calcination of mixed oxides was carried out at 923 K unless otherwise specified. The ternary mixed oxides have a molar composition of $Ce_{0.76}Zr_{0.19}M_{0.05}O_{2-x}$ (with M=Mn or Cu), where x stands for the number of $Mn^{3+/4+}$ or Cu^{2+} inserted, and accounts for the charge difference between M and Ce or Zr. Surface areas (BET method) were measured with a Sorptomatic Carlo Erba 1900 instrument. Quantitative temperature-programmed reduction (TPR) was carried out as previously detailed [10]. Structural characterization was executed with a Siemens X-ray diffraction unit by using Cu radiations. The position and the intensity of the diffraction lines have been calculated by fitting the experimental data with Voigt functions.

2.2. Catalytic tests

Catalytic tests were carried out with a micro flow reactor operating at steady state conditions. The powdered catalysts were sieved (100–200 μm) and loaded into a quartz reactor inserted in a furnace (Carbolite MTF12/25). The reaction mixture containing 1 mol% of alkane, 8% oxygen and balance helium (only in the case of CH_4, 4% oxygen was used) was fed to the reactor at a GHSV of 50 000 h^{-1} with a total flow rate of 100 ml/min (STP). The products were analysed with a HP5890 gaschromatograph equipped with two Porapack Q columns and TCD and FID detectors. To allow detection of CO and CO_2 with FID a methanator was inserted between one column and the FID.

3. Results and discussion

In Table 1 and Fig. 1 are summarized the textural and reduction properties of the $Ce_xZr_{1-x}O_2$ samples (with x varying from 1 to 0.5). Fig. 1 shows the TPR traces of solid solutions of an increasing Zr content. As can be seen the introduction of Zr strongly modifies the reduction behaviour of CeO_2. TPR of ceria shows two maxima at ca. 820 and 1100 K, which has been associated to surface and bulk reduction, respectively

Table 1
Textural and reduction properties of CeO_2–ZrO_2 solid solutions

Sample	Surface area (m^2/g)[a]	CeO_2 reduction[b] (%)	H_2 consumed[b] (ml/g)
CeO_2	52	15.6	11.0
$Ce_{0.92}Zr_{0.08}O_2$	94	19.0	12.7
$Ce_{0.8}Zr_{0.2}O_2$	93	26.4	15.9
$Ce_{0.65}Zr_{0.35}O_2$	85	29.5	15.0
$Ce_{0.5}Zr_{0.5}O_2$	87	44.6	18.5

[a]Measured after calcination at 823 K for 2 h.
[b]Calculated from TPR measurements of 900 K.

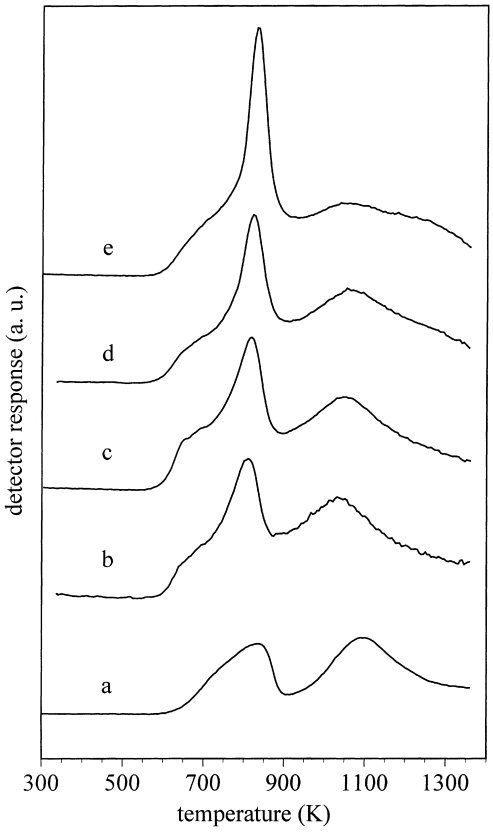

Fig. 1. TPR traces of (a) CeO_2, (b) $Ce_{0.92}Zr_{0.08}O_2$, (c) $Ce_{0.8}Zr_{0.2}O_2$, (d) $Ce_{0.65}Zr_{0.35}O_2$, and (e) $Ce_{0.5}Zr_{0.5}O_2$. For clarity the curves have been normalized.

[11]. With the introduction of an even relatively small amount of Zr, the reduction of Ce^{4+} is promoted and it is observed at lower temperatures with two maxima at ca. 800 (peak 1) and 1030–1050 K (peak 2) and a shoulder at ca. 650 K. Peak position is almost unaffected by increasing the amount of ZrO_2 from 8% to 50%, while a change in the intensity ratio (peak 1/peak 2) is observed, reaching a maximum with $Ce_{0.5}Zr_{0.5}O_2$. The corresponding reduction of CeO_2 in solid solutions is also increased with increasing Zr content (see Table 1); with $Ce_{0.5}Zr_{0.5}O_2$ more than 80% of the Ce^{4+} present has been reduced to Ce^{3+} at the final temperature of 1300 K. Although the percentage of reduced cerium increases by raising the Zr content, the overall H_2 consumption (on a per gram basis) is less affected in this composition range due to the amount of CeO_2 present, which is the factor limiting the total H_2 consumption. This is in agreement with what has been reported about metal-loaded, low-surface area ceria–zirconia solid solutions [5]; also in this case an enhancement of Ce^{4+} reduction was observed upon increasing the amount of Zr, up to the formation of $Ce_{0.5}Zr_{0.5}O_2$, where the highest degree of support reduction and lowest reduction temperatures were observed. The promotion of Ce^{4+} reduction can be related to a higher mobility and diffusion of bulk O_2 due to the creation of a defective structure by introduction of Zr into CeO_2 lattice. The presence of dopant increases the total amount of oxygen that can be reversibly exchanged between the solid and the surrounding atmosphere, and affects the kinetics of the redox processes by lowering the activation energy for hopping of oxygen, which in turn results also in a higher oxygen storage capacity [9]. Similar findings have also been found with CeO_2 doped with PrO_x [12,13] or other aliovalent oxides, like Gd_2O_5 [14] and La_2O_3 [15]. In all cases the results have been rationalized in terms of bulk and surface structural features of the mixed oxides which affect the redox processes.

To further promote the reduction behaviour, especially at lower temperature, we have used CeO_2–ZrO_2 as a base for preparing ternary mixed oxides containing small quantities of MnO_x and CuO. This choice is the result of several considerations: (i) both components (Mn and Cu), and especially Mn, posses an active redox behaviour, existing in several oxidation states [16]; (ii) the presence of CeO_2, in synergism with MnO_x and CuO, has been shown to promote oxygen mobility and redox activity [17,18]; (iii) if present in low amounts, both $Mn^{3+/4+}$ and Cu^{2+} can dissolve within the CeO_2 lattice, giving homogeneous solid solutions [19–21]; (iv) the activity in catalytic combustion could also benefit from the presence of MnO_x and CuO, which behave as active oxidation catalysts.

Structural features of solid solutions have been examined by XRD and HRTEM-EDX analysis. The X-ray diffraction pattern of Cu-doped CeO_2–ZrO_2 is shown in Fig. 2. The material crystallizes in a fluorite-like cubic phase. As can be seen from the figure, the shift of the diffraction peaks at higher Θ values with respect to pure, undoped ceria evidences a contraction of the cell parameter (a=5.357(7) Å vs. a=5.414(3) Å calculated for pure CeO_2). Particle size distribution is

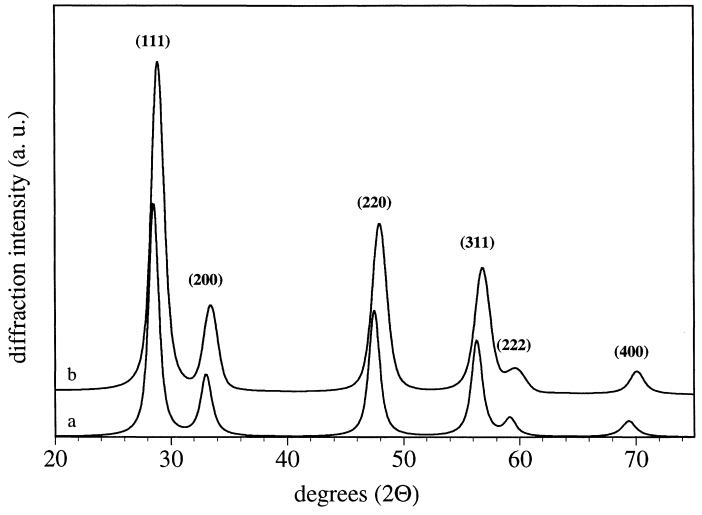

Fig. 2. X-ray diffraction profiles of (a) CeO_2, and (b) $Ce_{0.76}Zr_{0.19}Cu_{0.05}O_{2-x}$.

very narrow centred at around 5–6 nm. In no cases segregated phases of CuO, MnO_x, CeO_2 or ZrO_2 alone have been observed with EDX (spot size 5 nm). Also, X-ray diffraction analysis does not reveal the presence of single oxide phases, although at these low concentrations CuO or MnO_x might escape X-ray detection. Despite the fact that the ionic radius of Cu^{2+} and Mn^{4+} differs from that of Ce^{4+}, formation of fluorite-structured cubic solid solution with similar systems (MnO_x–CeO_2 [19], MnO_x–ZrO_2 [20], CuO–CeO_2 [21]) has also been reported, showing that at low dopant concentration both MnO_x and CuO can dissolve within CeO_2 and ZrO_2 lattices. Surface areas measured after calcination at different temperatures indicate a marked difference in the textural properties between CeO_2 and the mixed oxides (see Fig. 3). This is true especially for CeO_2–ZrO_2, which seems to have the best resistance to high-temperature treatments. The introduction of Cu and Mn does not seem to further improve the thermal resistance, particularly in the temperature range >1000 K where undoped ceria–zirconia shows the better behaviour.

In Fig. 4 are reported the TPR traces of Mn and Cu-containing samples; for comparison TPR profiles of $Ce_{0.8}Zr_{0.2}O_2$ and of CuO and various MnO_x are also included. The introduction of these dopants strongly modifies the TPR profile of pure CeO_2–ZrO_2. In particular low-temperature features attributable to reduction of Cu^{2+} to Cu and of $Mn^{3+/4+}$ to Mn^{2+} were observed. Quantitative calculations on the amount of H_2 consumed in the TPR of CuO and MnO_x show that Cu and Mn^{2+} (as MnO) are the final state after reduction. Consistently a TPR of pure MnO shows no H_2 consumption in the temperature range investigated. With $Ce_{0.76}Zr_{0.19}Mn_{0.05}O_{2-x}$ the onset of Mn reduction at ca. 480 K is more than 100 K lower than that of Mn in MnO_2, Mn_3O_4 and Mn_2O_3. This behaviour can be attributed to the higher surface area in mixed oxides as compared to pure MnO_x. In addition, the presence of Ce can modify the redox activity of Mn, by stabilizing Mn in higher oxidation states at low temperatures and by facilitating the migration of oxygen from Mn, as the temperature is increased [17]. The promotion of low-temperature redox behaviour is even more pronounced with CuO containing materials. The onset of H_2 uptake is observed at 378 K with a maximum at 483 K. By integrating the TPR curve, in correspondence of the low-temperature signal, a H_2 consumption of 660 μmol/g is observed which exceeds that required for reduction of the CuO present in the sample. Therefore a substantial amount of Ce^{4+} is also reduced at these low temperatures; a behaviour which is similar to that observed with CeO_2-supported noble metals [3]. In parallel with the reduction of Cu^{2+} and Ce^{4+} a possible consumption of H_2 due to incorporation and storing of H_2 into the lattice, as described by Wrobel et al. [22], is likely to take place. The synergism between formation of H-species into the

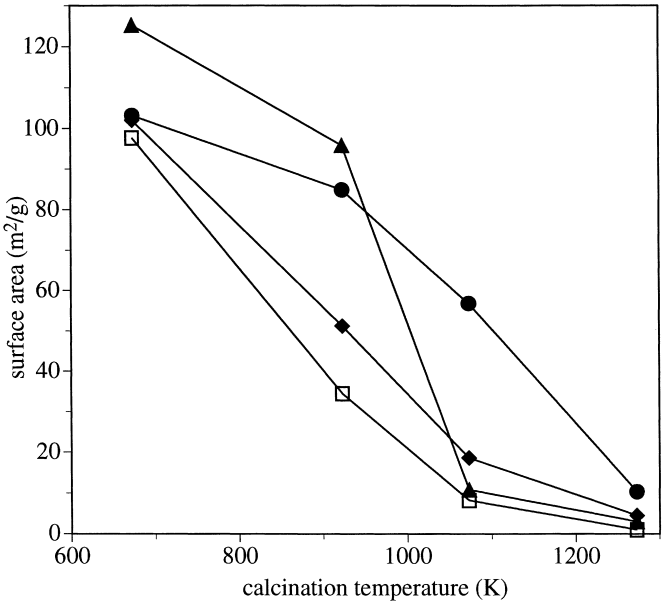

Fig. 3. Surface area at different calcination temperatures: (□) CeO_2, (●) $Ce_{0.8}Zr_{0.2}O_2$, (◆) $Ce_{0.76}Zr_{0.19}Mn_{0.05}O_{2-x}$, and (▲) $Ce_{0.76}Zr_{0.19}Cu_{0.05}O_{2-x}$. Catalysts (0.5 g) were held for 2 h at the temperature indicated under air flow (150 ml/min).

lattice and reduction of host cation according to Wrobel et al. [22] could also contribute to the enhancement of Ce^{4+} reduction at lower temperatures.

Another interesting feature, which is observed in these systems, is the stability under repeated redox cycles. In Fig. 5 are reported the TPR of a binary Mn–Ce–O and ternary Mn–Ce–Zr–O mixed oxide for the fresh catalysts and for the catalysts recycled once, i.e. subjected to repeated reduction/oxidation/reduction treatments. The low-temperature redox activity is almost completely lost in the binary system after the first TPR, while the redox behaviour at low temperature holds for the ternary oxide, despite the thermal treatment at 1400 K, with a corresponding decrease in surface area. This behaviour is attributable to the presence of ZrO_2, which promotes the reduction at low temperatures even with materials having low surface areas [5–7,9].

The results concerning catalytic activity are reported in Figs. 6 and 7 for methane oxidation, while Table 2 summarizes the activity in the combustion of the other hydrocarbons tested. In Fig. 6 the catalytic activity of various CeO_2–ZrO_2 mixed oxides is compared using the temperature of 50% conversion; in addition values for Mn and Cu-doped samples are included. The efficiency increases upon decreasing the amount of Zr and reaches a maximum with $Ce_{0.92}Zr_{0.08}O_2$. It seems that this behaviour could

Table 2
Catalytic combustion of alkanes (ethane, propane, butane and isobutane) over Cu and Mn-doped ceria–zirconia[a]

	C_2H_6		C_3H_8		C_4H_{10}		iC_4H_{10}	
	$T_{50\%}$ (K)	$T_{90\%}$ (K)	$T_{50\%}$	$T_{90\%}$	$T_{50\%}$	$T_{90\%}$	$T_{50\%}$	$T_{90\%}$
CeO_2	783	919	758	906	736	842	730	836
$Ce_{0.8}Zr_{0.2}O_2$	768	848	731	813	710	802	710	786
$Ce_{0.76}Zr_{0.19}Mn_{0.05}O_{2-x}$	727	827	681	765	667	756	651	749
$Ce_{0.76}Zr_{0.19}Cu_{0.05}O_{2-x}$	704	806	685	762	652	734	641	727

[a]Conditions as specified in Section 2. Catalysts were aged in air at 923 K for 2 h before use.

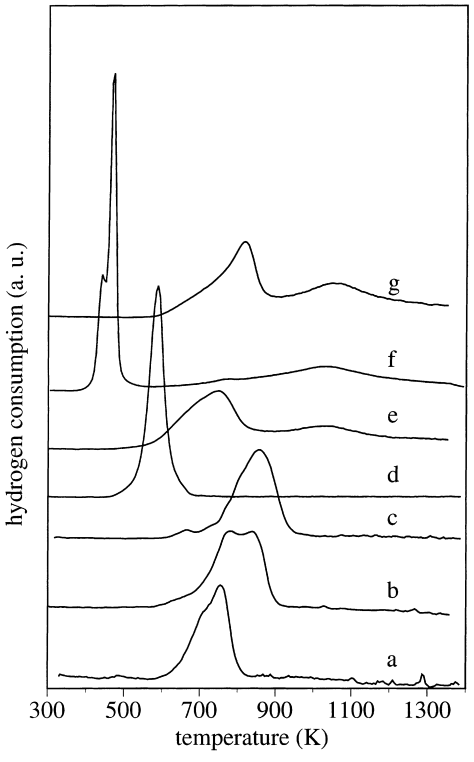

Fig. 4. TPR profiles of (a) Mn_3O_4, (b) Mn_2O_3, (c) MnO_2, (d) CuO, (e) $Ce_{0.76}Zr_{0.19}Mn_{0.05}O_{2-x}$, (f) $Ce_{0.76}Zr_{0.19}Cu_{0.05}O_{2-x}$, and (g) $Ce_{0.8}Zr_{0.2}O_2$.

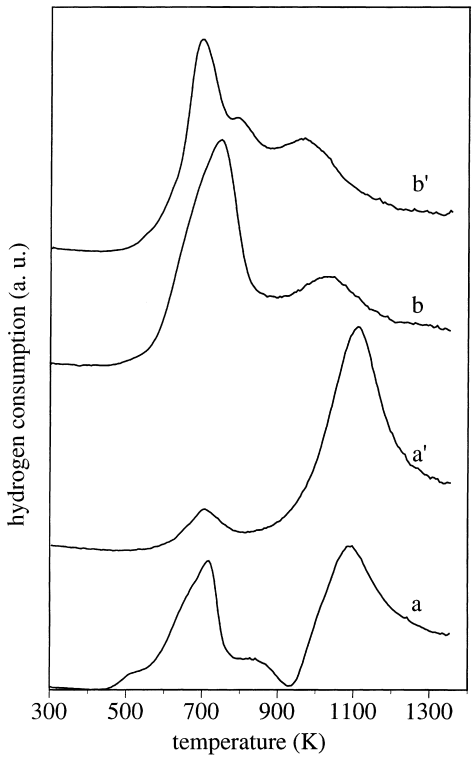

Fig. 5. TPR profile of (a) $Ce_{0.95}Mn_{0.05}O_{2-x}$, (a′) sample (a) recycled once after TPR and reoxidation at 773 K, (b) $Ce_{0.76}Zr_{0.19}Mn_{0.05}O_{2-x}$, (b′) sample (b) recycled once.

be correlated with structural features rather than surface area, although the amount of acid/base sites present on the surface of modified ceria could play an important role in the heterolytic activation of C–H bond of CH_4 [23]. It has been observed that with Ce–Zr and similar systems the oxygen mobility is strongly dependent on structural features (for example, the cubic phase favours oxygen diffusion in Ce–Zr–O system as compared to the tetragonal phase [5]) and on the abundance of the redox element in the mixture [12,13]. A high concentration of Ce in this case would accelerate the process of oxygen transfer through the lattice. Therefore it seems that the maximum of activity could be correlated with a higher effectiveness in the diffusion of oxygen through the lattice; in the present case, among the samples investigated, cubic $Ce_xZr_{1-x}O_2$ (with $x>0.8$) are favoured as compared to samples with a lower Ce content ($0.5<x<0.8$).

The introduction of Cu and Mn further promotes the activity by lowering the light-off temperature. In Fig. 7 is also reported the effect of the amount of Mn in solid solution with CeO_2–ZrO_2. There are no large variations in the activity of Mn-containing catalysts, although $Ce_{0.76}Zr_{0.19}Mn_yO_{2-x}$, with $y=0.05$, behaves slightly better if compared to samples with $y=0.1$ and 0.025. This points out that it is not only the total amount of dopant that drives the activity in this composition range, but an equilibrium between the different components of the mixture. Similar results are obtained with the oxidation of other hydrocarbons (Table 2). The order of activity is Cu–Ce–Zr–O>Mn–Ce–Zr–O>Ce–Zr–O>CeO_2. In this case the effect of adding Mn and Cu is much more evident than with methane; the difference in the light-off temperatures ranges between 45 and 70 K. The reaction conditions here (especially low temperature) may favour the reactivity of catalysts whose redox behaviour is promoted at low temperature.

In conclusion it seems that what makes doped ceria more active is the increase of oxygen mobility which

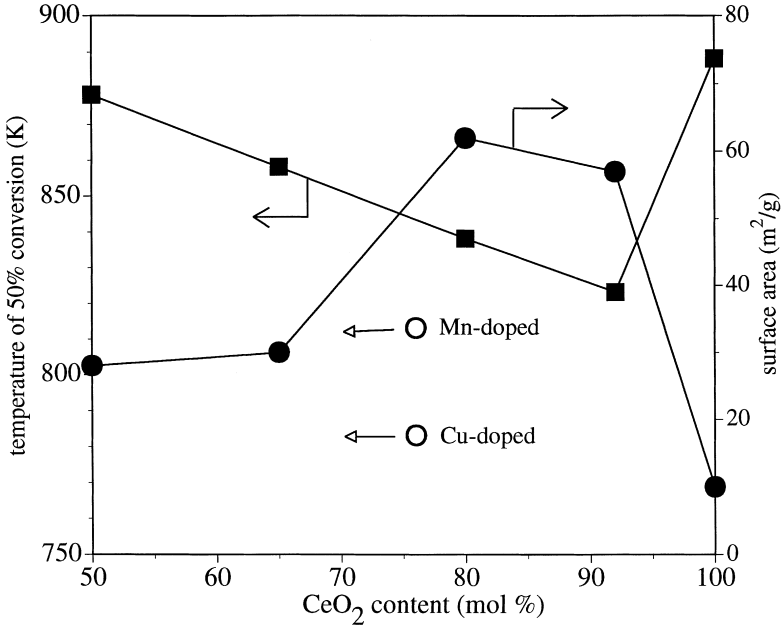

Fig. 6. Temperature of 50% conversion and surface area (after calcination at 1073 K) vs. CeO_2 content (mol%) in CeO_2–ZrO_2 solid solutions. (■) $T_{50\%}$, (●) surface area, and (○) $T_{50\%}$ for Mn and Cu-doped catalysts is also indicated.

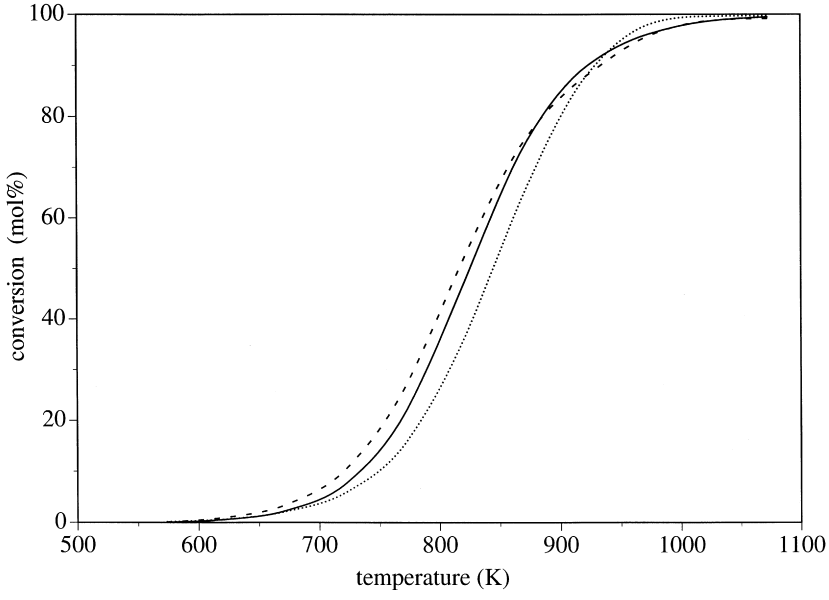

Fig. 7. Catalytic activity in methane combustion of $Ce_{0.76}Zr_{0.24-y}Mn_yO_{2-x}$ catalysts: (——) y=0.1, (— — —) y=0.05, and (· · · · · ·) y=0.025.

is the result of introduction of defect sites. In the case of CeO_2–ZrO_2 these defect sites are introduced by a redox process, while with Mn and Cu-doped CeO_2–ZrO_2, due to the presence of elements of a different charge, ionic defects are created by a charge compensation mechanism. Moreover, catalytic activity could

also take advantages from the oxidation ability of Mn and Cu and their redox efficiency at low temperature. The presence of Zr seems to be important especially for stabilizing redox activity against surface area loss, which might be necessary in high-temperature applications.

References

[1] M.F.M. Zwinkels, S.V. Jaras, P.G. Menon, T.A. Griffin, Catal. Rev.-Sci. Eng. 35(3) (1993) 319.
[2] J.J. Spivey, Ind. Eng. Chem. Res. 26 (1987) 2165.
[3] A. Trovarelli, Catal. Rev.-Sci. Eng. 38(4) (1996) 439.
[4] F. Zamar, A. Trovarelli, C. de Leitenburg, G. Dolcetti, J. Chem. Soc., Chem. Commun. (1995) 965.
[5] P. Fornasiero, R. Di Monte, G.R. Rao, J. Kaspar, S. Meriani, A. Trovarelli, M. Graziani, J. Catal. 151 (1995) 168.
[6] F. Zamar, A. Trovarelli, C. de Leitenburg, G. Dolcetti, Stud. Surf. Sci. Catal. 101 (1996) 1283.
[7] G. Balducci, P. Fornasiero, R. Di Monte, J. Kaspar, S. Meriani, M. Graziani, Catal. Lett. 33 (1995) 193.
[8] M. Pijolat, M. Prin, M. Soustelle, O. Touret, P. Nortier, J. Chem. Soc., Faraday Trans. 91 (1995) 3941.
[9] C. de Leitenburg, A. Trovarelli, G. Bini, F. Cavani, J. Llorca, Appl. Catal. A 139 (1996) 161.
[10] A. Trovarelli, C. de Leitenburg, G. Dolcetti, J. Llorca, J. Catal. 151 (1995) 111.
[11] H.C. Yao, Y.F.Y. Yao, J. Catal. 86 (1984) 254.
[12] A.D. Logan, M. Shelef, J. Mater. Res. 9 (1994) 468.
[13] M.Yu. Sinev, G.W. Graham, L.P. Haach, M. Shelef, J. Mater. Res. 11 (1996) 1960.
[14] B.K. Cho, J. Catal. 131 (1991) 74.
[15] T. Miki, T. Ogawa, M. Haneda, N. Kakuta, A. Ueno, S. Tateishi, S. Matsura, M. Sato, J. Phys. Chem. 94 (1990) 6464.
[16] F. Kapteijn, L. Singoredjo, A. Andreini, J.A. Moulijn, Appl. Catal. B 3 (1994) 173.
[17] S. Imamura, M. Shono, N. Okamoto, A. Hamada, S. Ishida, Appl. Catal. A 142 (1996) 279.
[18] S. Kacimi, J. Barbier Jr., R. Taha, D. Duprez, Catal. Lett. 22 (1993) 343.
[19] Y. Zhang, A. Andersson, M. Muhammed, Appl. Catal. B 6 (1995) 325.
[20] A. Keshavaraja, A.V. Ramaswamy, J. Mater. Res. 9 (1994) 837.
[21] C. Lamonier, A. Bennani, A. D'Huysser, A. Aboukaïs, G. Wrobel, J. Chem. Soc., Faraday Trans. 92 (1996) 131.
[22] G. Wrobel, C. Lamonier, A. Bennani, A. D'Huysser, A. Aboukaïs, J. Chem. Soc., Faraday Trans. 92 (1996) 2001.
[23] W. Liu, M. Flytzani-Stephanopoulos, J. Catal. 153 (1995) 317.